

Contents lists available at ScienceDirect

Acta Materialia

journal homepage: www.elsevier.com/locate/actamat



Full length article

Stishovite nucleation at low shock pressures in soda-lime glass

Pratyush Srivastava^a, Koichi Tanaka^b, Brian Ramirez^c, Vijay Gupta^{a,b,*}

- ^a Department of Mechanical and Aerospace Engineering, University of California Los Angeles, Los Angeles, CA 90095, USA
- ^b Department of Materials Science and Engineering, University of California Los Angeles, Los Angeles, CA 90095, USA
- ^c Department of Mechanical Engineering, California State Polytechnic University, Pomona, CA 91768, USA



ARTICLE INFO

Article history: Received 26 December 2020 Revised 17 June 2021 Accepted 21 June 2021 Available online 26 June 2021

Keywords: Soda-lime glass Shock compression High resolution TEM Phase transformation Crystallization

ABSTRACT

Highly dense and ultra-hard Stishovite phase is the most stable form of SiO_2 . It is formed when fused silica is subjected to extreme pressures (>34 GPa). In this communication, we report nucleation of the Stishovite phase in shock-loaded soda-lime glass (SLG) samples at a remarkably low compressive stress of 7 GPa. Although it falls within the reported Hugoniot Elastic Limit of SLG between 2.5 and 7 GPa, it is significantly below the crystallization threshold of 34 GPa observed for fused silica. SLG plates were shock loaded by impacting them at 1–2.5 km/s using a table-top experimental setup in which 1 mm-dia Al micro flyer plates of 25–50 μ m thickness were generated and propelled using a top-hat Nd:YAG laser pulse of 8 ns duration. The shocked samples were imaged using High Resolution Transmission Electron Microscopy (HRTEM) and further analyzed using Selected Area Electron Diffraction and FFT analyses. All samples showed nucleation of 4 nm Stishovite crystals distributed within the amorphous SLG matrix. The stress state was determined by directly measuring the flyer speed, particle velocity, and shockwave speed by using a state-of-the-art Photonic Doppler Velocimeter (PDV).

 $\ensuremath{\mathbb{C}}$ 2021 Acta Materialia Inc. Published by Elsevier Ltd. All rights reserved.

1. Introduction

Recently the shock response of soda-lime glass (SLG) has received much attention in the armor research community because of its potential to absorb substantial shockwave energy by transforming into its crystalline Stishovite phase. This phase transformation is accompanied by almost 40% volume reduction and is similar to that uncovered in silica glasses. Barsoum et al. [1] subjected a stack of SLG layers to a hypervelocity penetrator and analyzed the debris left behind in the channel created by the projectile. Prior to the X-ray analysis, the debris was washed in a hydrofluoric acid bath in which the Stishovite phase dissolves very poorly. The analysis confirmed the formation of the Stishovite phase. By subjecting SLG samples to shock pressures up to 110 GPa, Gorfain et al. [2] found that the high pressure Hugoniot of SLG displayed stiffness that was similar to that of pure Stishovite. Alexander et al. [3] measured the release response of SLG from pressures as high as 40 GPa and observed a change in the shock release dynamics when compared to the fused silica response. Their work suggested that the network modification of silica due to the presence of alkali oxides in SLG inhibits transition to the Stishovite phase.

However, the high-pressure steepness in the Hugoniot curve, similar to Stishovite hydrostat, suggested a quick reversible transition that prevents freezing of the Stishovite phase. In all of these previous studies the entire volume of the sample is transformed into the crystalline phase which is then spotted through the change in continuum-level mechanical response. However, among recent studies on shock response of SLG, Renganathan et al. [4] provided a different picture of continuum response at high stress levels (37–120 GPa). The linear shock velocity – particle velocity $(U_s - u_n)$ model in their study shows that the Hugoniot states do not match the stiffness of the Stishovite phase as observed in fused silica. The aim of our research leading to this paper was to determine the threshold stress state at which the Stishovite crystals are nucleated from the amorphous SLG phase. The continuum Hugoniot response is not sensitive enough to spot the onset of any crystalline transformation. We determined the Stishovite nucleation stress by subjecting a series of SLG glass plates to increasing stress amplitudes from well-defined rectangular stress pulses of 8 and 16 ns duration. These stress pulses were generated by impacting the samples by laser-generated and propelled microflyer plates at 1-2.5 km/s. Each shocked sample was then carefully analyzed using a combination of atomic resolution Transmission Electron Microscopy and FFT analysis to spot for any nucleated Stishovite nanocrystals. In this paper, we report the formation of Stishovite crystals of 4 nm in size at a threshold stress of 7 GPa which is above its lowest reported Hugoniot Elastic Limit of 2.5 GPa [5].

^{*} Corresponding author at: Department of Mechanical and Aerospace Engineering, University of California Los Angeles, Los Angeles, CA 90095, USA E-mail address: vgupta@ucla.edu (V. Gupta).

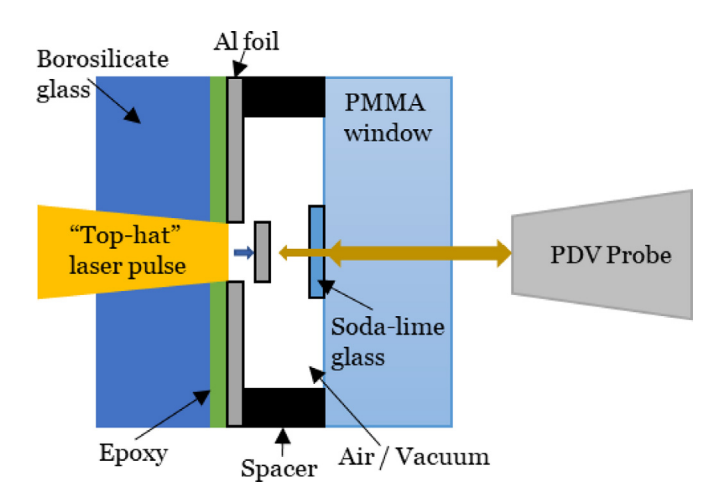


Fig. 1. Cross-sectional view of the sample assembly showing punching of the flyer disc by the impinging top-hat laser pulse, and the probe beam from PDV for measuring the flyer velocity and shock arrival at the sample's back surface.

These results are in accord with our previously reported results under quasi-static conditions where Stishovite nanocrystals were found to nucleate at a peak nominal stress of only ~5 GPa in SLG nanopillars that were compressed *in-situ* using a picoindenter stationed inside a scanning electron microscope [6]. The very low nucleation stress was attributed to the presence of very high shear stresses (~2.5 GPa) that resulted in the diffusion of Na⁺ and Ca²⁺ ions to create local regions of pure SiO₂ where nanocrystal nucleation was found to occur.

2. Experimental setup and procedure

A cross-sectional view of the sample assembly that was used to load SLG plates by an Al microflyer plate is shown in Fig. 1. The micro flyer plate was generated by impinging a 8 ns duration, Nd:YAG laser pulse, onto a 1 mm diameter spot on the back surface of a 25 µm thick Al foil which was bonded to a transparent borosilicate glass window of 6 mm thickness. The absorbed optical radiation at the foil's rear surface creates plasma and leads to punching out of an aluminum microflyer disc of approximately the laser-impinging diameter [7]. This microflyer disc then accelerates through the air (or vacuum) due to the rapid expansion of the plasma on its rear surface and impacts the SLG sample that is stationed about 500 µm in front. The flyer plate attains its maximum velocity within 100 ns. To create space for the accelerating flyer, the SLG sample was axially separated from the glass window by using edge spacers. The entire assembly was secured inside a sample holder (Fig. 2). A Nd:YAG pulse laser of 2 J max energy and 12 mm output beam diameter was used as the launch laser. Following the procedure outlined by Brown et al. [7], the output pulse from the YAG laser with a Gaussian energy profile with a M² value of 2 was first converted into a "top-hat" beam using diffractive optics. The top-hat beam output was then focused on the back surface of the Al foil using an aspheric lens. This is an important part of the experimental procedure because the use of a Gaussian profile pulse results in the generation of non-uniform spatial stresses within the flyer plate volume and results in its complete disintegration prior to its arrival at the SLG target. The top-hat beam has a significant number of hot spots in its profile but they were found not to affect the launch and the planarity of the flyer plate [7].

The stress state, σ , in the sample was obtained by measuring the flyer velocity, particle velocity up at the sample's back surface (that is struck by the flyer plate), and the shock velocity U_s through the sample, by using a state-of-the-art Photonic Doppler Velocimeter (PDV). A schematic of the PDV along with other optical compo-

nents that were used in training the interferometric and the launch laser beams, to and from the sample surface, are shown in Fig. 2. Details of PDV construction and its working principle can be found in the literature [8,9]. In our study, a combination of GRIN collimator and a microscope objective was used as the probe. The PDV beam from the 1550 nm CW laser source (Fig. 2) was first collimated to 500 μm diameter and then focused onto the front surface of the Al foil using an objective lens. The focused spot was ~78 μm with a long Rayleigh length of about 12 mm. This arrangement ensured that the microflyer disc remained in focus during its entire flight distance of 500 μm before it struck the SLG sample. The pulse and the probe beams were perfectly aligned using lasers to ensure that the probe beam was focused right at the center of the launched microflyer plate.

The stress, σ , in the sample was calculated using,

$$\sigma = \rho_0 U_{\rm s} u_{\rm p} \tag{1}$$

Here, ρ_0 is the initial density of the sample. The particle velocity (u_p) was taken as the velocity of the flyer plate immediately after the impact. The transparency of the SLG sample allowed simultaneous measurements of the flyer velocity and the shock velocity. This was accomplished by coating the front (PDV) side of the SLG sample with a semi-transparent Au layer of 15 nm thickness [10]. As shown in Fig. 2, the transmitted part of the PDV beam tracked the movement of the flyer while the part that was reflected by the Au layer detected the arrival of shockwave at the front surface of the sample. With known sample thickness, this allowed accurate determination of the shock velocity through the sample.

Tests were performed using 25 μ m and 50 μ m thick flyer plates which resulted in stress pulses of 8 ns and 16 ns duration, respectively. These flyer plates were launched with 50–150 J/cm² laser fluence which resulted in a peak flyer velocity of 2.5 km/s.

3. Results and discussion

Fig. 3(a,c) show PDV signals that were acquired when SLG plates were struck with 25 μ m thick and 50 μ m thick flyer plates, respectively. Both these flyers were propelled using a laser fluence of 100 J/cm^2 . Fig. 3(b,d) show the corresponding velocity spectrograms that were obtained after reducing the raw data in Fig. 3(a,c), respectively, by using the moving window Fourier transform routine. As seen in Fig. 3(b,d), there is a sudden drop in the flyer's velocity which corresponds to the time of impact with the sample. The planar shock generated in the sample can be observed in the spectrogram as the period of constant velocity immediately after the impact. This was recorded as the particle velocity, u_p . Consistent with the standard flyer plate setups, the generated shockwave in the sample has a duration that is equal to the shockwave round trip time in the microflyer plate, which is 8 ns and 16 ns, for the 25 μ m and 50 μ m thick flyer plates, respectively.

The Hugoniot equation of state results for SLG from our impact experiments are shown in Fig. 4 along with those obtained using the conventional gas-gun launched plate impact setups from the literature. The maximum shock pressure achieved in our tests was 22 GPa which corresponded to the micro flyer impact velocity of 2.5 km/s. Our micro flyer data tracks data from other investigators fairly well. However, our data is at strain rates $(10^7-10^8 \text{ s}^{-1})$ that are about two orders of magnitude higher. It should be noted that we can take hundreds of shots in a single day, if needed. In contrast, in traditional plate impact setups, one is limited to no more than 10 shots per day because of the complexities associated with reloading the multi-stage gas guns. Another advantage of the micro flyer impact setup is that the glass sample remains intact after impact as the damage is localized to only 1 mm-dia region of the 25 mm-diameter glass plate. This allows microscopic examination of the severely deformed and micro-cracked region of the otherP. Srivastava, K. Tanaka, B. Ramirez et al. Acta Materialia 215 (2021) 117124

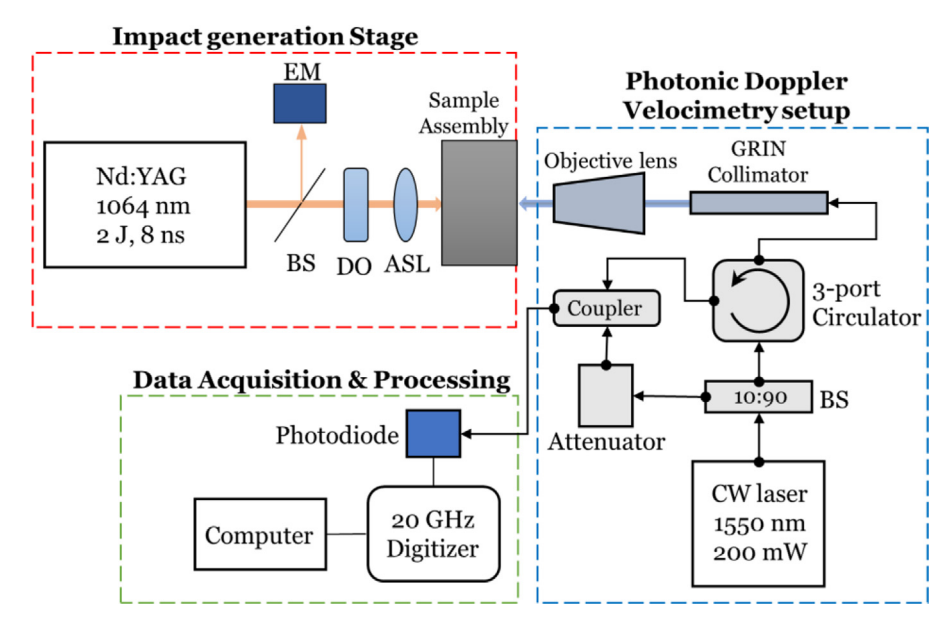


Fig. 2. Schematic of the laser generated flyer plate setup along with that of the Photonic Doppler Velocimeter (PDV). EM = Energy Meter, BS = Beam Splitter, DO = Diffractive Optic, ASL = Aspheric Lens, CW = Continuous Wave. Black arrows in PDV setup denote single-mode optical fibers for 1550 nm wavelength.

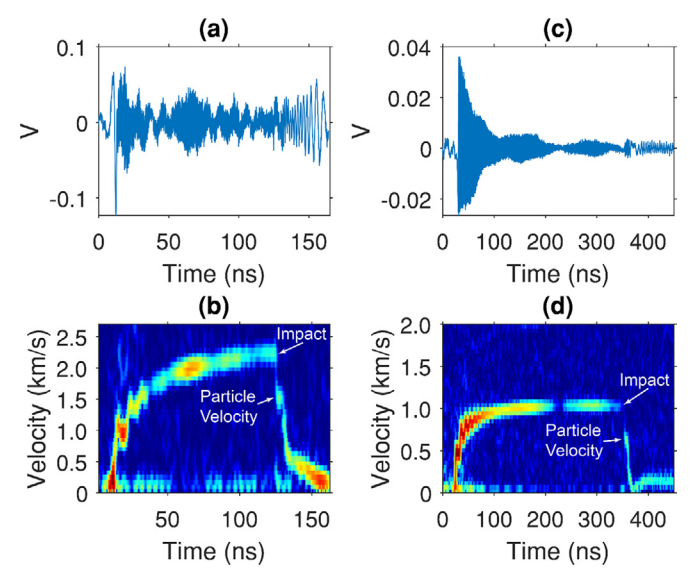


Fig. 3. Representative PDV signals for flyers launched at 100 J/cm^2 laser fluence. (a) and (b) Display the probe signal and its corresponding spectrogram, respectively, for a 25 µm flyer, whereas (c) and (d) show the same for a 50 µm flyer that was launched with the same laser fluence. Point of abrupt drop in the velocity spectrogram coincides with the flyer impact (shown via arrow). The short duration of constant velocity (particle velocity shown via arrow) following the flyer impact represents the period of shock generation in the sample.

wise intact plate. Fig. 5(a-c) show the results of such an analysis for a crater that was caused by a 50 μ m thick flyer disc. This sample was subjected to 1.0 km/s impact, resulting in a peak pressure of 7 GPa for 16 ns. A summary of the impact experiments is shown in Table 1.

To spot for any polymorphic changes, the microstructures of the samples that were shocked to 7, 10 and 20 GPa pressure were examined using a FEI-Titan Scanning/Transmission Electron Microscope (STEM) at 300 kV. The TEM specimens were prepared from the center of the impacted region by FIB micromachining as shown in Fig. 5(d-f). Atomic-scale imaging and Fast Fourier Transform (FFT) analyses confirmed the presence of nanocrystalline regions, about 4 nm in size, distributed within an amorphous matrix. These

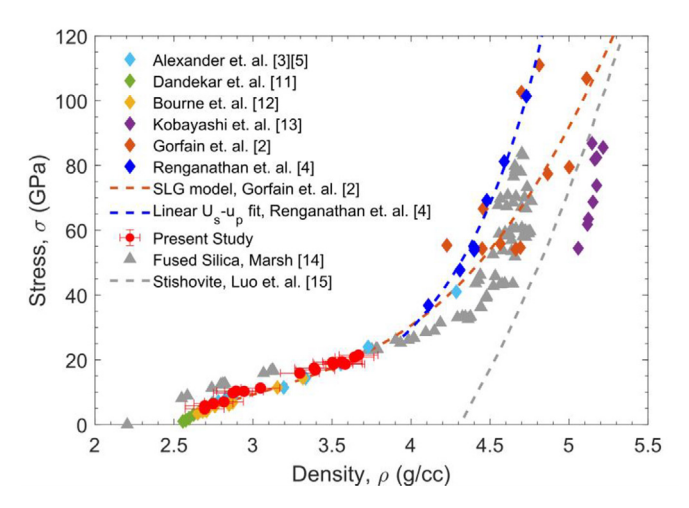


Fig. 4. Shock Hugoniot curve for Soda-lime glass (SLG) taken from [2, 3, 4, 5, 11, 12, 13]. Red circles with error bars represent the results from the present study. Strain rate was $1.25 \times 10^8 \text{ s}^{-1}$. Hugoniot for fused silica and pure Stishovite obtained by various investigators [14, 15] are also shown for comparison.

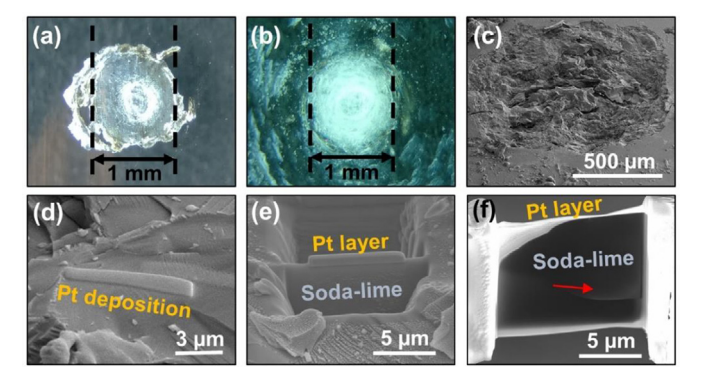


Fig. 5. (a) Optical micrograph showing a recovered 50 μ m thick flyer disc. It impacted the sample at 1.0 km/s to result in a planar shock pressure of 7 GPa for a duration of 16 ns. Optical (b) and SEM (c) images of the impact site on the sample. (d), (e), and (f) Show TEM sample preparation steps using FIB. Red arrow in (f) points to region where HRTEM images were taken (For interpretation of the references to color in this figure legend, the reader is referred to the web version of this article.).

Table 1 Summary of laser generated flyer plate impact experiments on SLG samples. Flyer, particle, and shock velocities were measured directly using the PDV. The stress and density values were calculated using the Hugoniot relations. Experiment (Expt.) number (No.) starting with designation fp25 and f50 correspond to flyer plates of thickness 25 μ m and 50 μ m, respectively.

Expt. No.	Flyer Velocity (km/s)	Peak Particle Velocity u _p (km/s)	Shock Velocity U _s (km/s)	Peak Stress σ (GPa)	Density ρ (g/cm ³)
fp50-700	0.68	0.41 ± 0.01	5.62 ± 0.20	5.81 ± 0.26	2.70 ± 0.12
fp50-1000	0.94	0.59 ± 0.01	4.77 ± 0.20	7.03 ± 0.29	2.82 ± 0.12
fp25-750	1.47	0.90 ± 0.01	5.00 ± 0.20	11.27 ± 0.43	3.05 ± 0.12
fp25-1000	2.01	1.24 ± 0.01	5.12 ± 0.20	15.88 ± 0.60	3.30 ± 0.12
fp25-1100	2.11	1.34 ± 0.01	5.05 ± 0.20	16.85 ± 0.64	3.39 ± 0.13
fp25-1100-1	2.11	1.36 ± 0.01	5.16 ± 0.20	17.45 ± 0.66	3.39 ± 0.13
fp25-1100-2	2.18	1.47 ± 0.01	5.09 ± 0.20	18.65 ± 0.70	3.51 ± 0.13
fp25-1200	2.30	1.51 ± 0.01	5.01 ± 0.20	18.83 ± 0.71	3.57 ± 0.13
fp25-1200-1	2.22	1.49 ± 0.01	5.18 ± 0.20	19.22 ± 0.72	3.50 ± 0.13
fp25-1200-2	2.46	1.62 ± 0.01	5.15 ± 0.20	20.81 ± 0.78	3.64 ± 0.14
fp25-1200-3	2.51	1.69 ± 0.01	5.19 ± 0.20	21.90 ± 0.80	3.67 ± 0.14

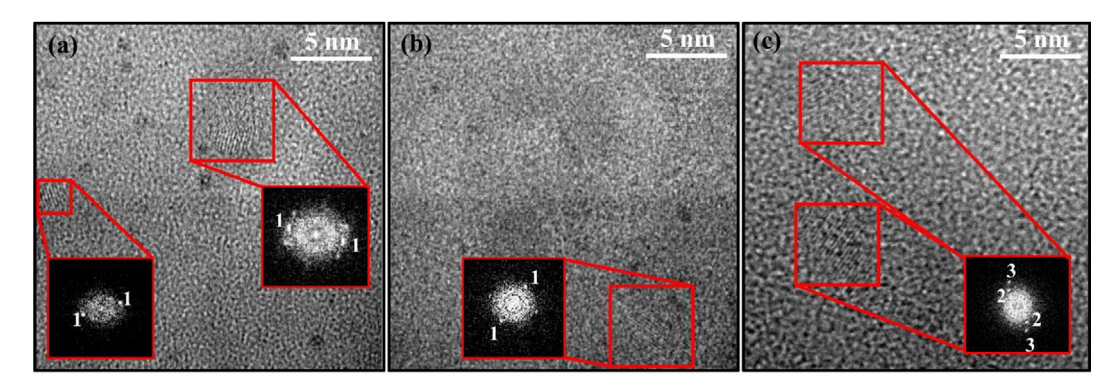


Fig. 6. HRTEM images of nucleated Stishovite crystals of approximate 4 nm in size in a series of Soda-lime glass samples that were subjected to planar shock pressures (duration in parenthesis) of (a) 7 GPa (16 ns), (b) 10 GPa (8 ns), and (c) 20 GPa (8 ns), resulting from impact velocities of 1.0 km/s, 1.5 km/s, and 2.5 km/s, respectively. HRTEM images were taken from near the bottom region of the respective samples, similar to that marked in Fig. 5f. The insets show FFT images of the nanocrystals, with diffraction spots (marked as 1, 2 and 3, with reference to Table 2) which were all confirmed to correspond to the Stishovite phase.

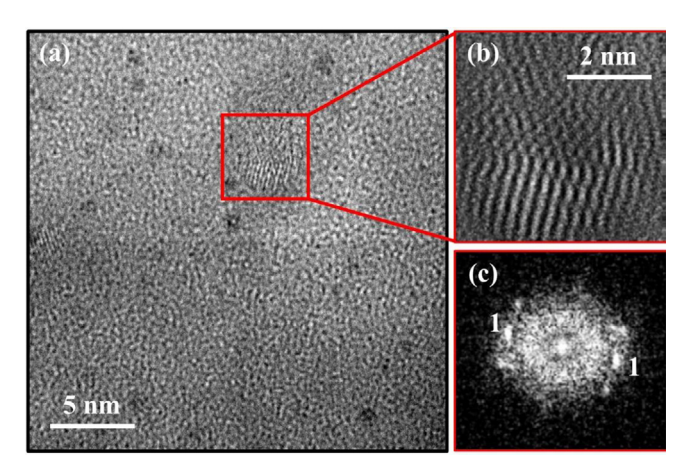


Fig. 7. Stishovite nucleation in the soda-lime glass sample of Fig. 5 that was subjected to 7 GPa pressure for 16 ns. (a) High resolution TEM image from the region marked with a red arrow in Fig. 5(f), showing crystalline regions distributed within an amorphous SLG matrix. (b) Zoomed-in image of one of the nanocrystals of 4 nm size. (c) FFT analysis of the region shown in (b) with diffraction spots marked as 1 (Table 2) which corresponds to a d-spacing value of 0.29 nm for Stishovite.

were found in all samples. Such regions from each sample are shown in Fig. 6. The indexed FFT results from one such region from a sample that was shocked to 7 GPa is shown in Fig. 7. It shows diffraction spots corresponding to the crystalline phase, in addition to the amorphous rings. The experimentally measured interplanar d-spacing from this analysis matched closely with those known in

Table 2 Interplanar (d) spacings measured from FFT analysis and its comparison with the known values for Stishovite from the literature. The index numbers refer to the ones shown in Figs. 6 and 7.

#	d measured (nm)	d Stishovite (nm)	hkl	Int.	Error (%)
1	0.29	0.2958	110	100	2.0
2	0.22	0.2249	011	22	2.2
3	0.15	0.1531	121	37	2.0

the literature for tetragonal Stishovite. Table 2 shows such a comparison. The very small difference between the two confirms these nanocrystalline regions to be that of Stishovite.

To rule out any electron beam irradiation related crystallization effects, as known in Si [16], we performed a control test by exposing SLG samples to 300 kV electron beam for 0, 7 and 12 min. The TEM examination of these samples did not reveal any crystalline phase as shown in Fig. 8.

4. Discussion

Our results provide first visual confirmation of Stishovite crystallization from amorphous SLG microstructure at extremely low shock pressure of 7 GPa. This is similar to our results obtained under quasi-static loading where Stishovite nucleation was observed between 5 and 6 GPa in uniaxially compressed SLG micro-pillars using a nanoindenter [6]. While these pressures are still above the Hugoniot elastic limit (HEL) [3-5,12] they are significantly below the 34 GPa threshold for transformation to the Stishovite phase

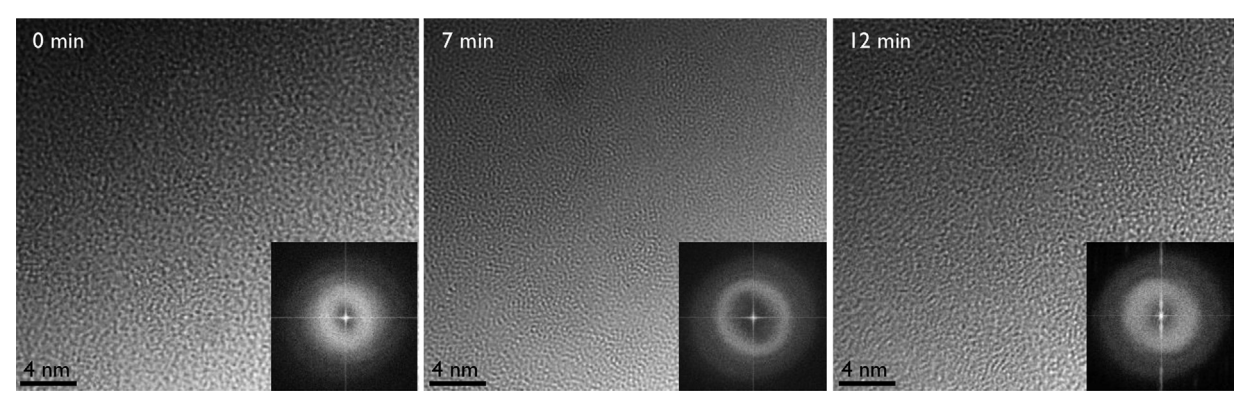


Fig. 8. TEM images along with their FFT analysis results (insets) for three bulk soda-lime glass samples that were exposed to electron beam for 0, 7 and 12 min. No crystalline phase is observed in any sample. These results prove that the crystalline phases found in the shock-loaded SLG samples are not due to any electron beam irradiation effect.

from fused silica as reported in a recent conclusive study of Tracy et al. [17]. Recognizing that the *in-situ* XRD analysis performed during the shock loading in the Tracy et al. study is not sensitive enough to record the nucleation of small number of Stishovite nanocrystals, we repeated the micro flyer experiments by replacing the SLG plates by fused silica plates of identical dimensions. The subsequent TEM and FFT analyses did not reveal nucleation of any Stishovite nanocrystals even when the samples were stressed to 20 GPa.

We are unable to directly compare our observations of very low Stishovite nucleation stress to any prior experimental or simulation studies on SLG. The low stress may be related to the known unusual elastic-plastic response of SLG compared to other materials. Sundaram and Clifton [18,19] and Clifton et al. [20] have reported a drop in shear resistance of SLG for longitudinal compressive stress greater than 3.5 GPa. Measurements by Alexander et al. [5] indicate that the longitudinal stress remains elastic up to 7.5 GPa despite a loss of shear resistance (strength) around 3.5 GPa. Applying the standard definition that the HEL is the stress at which a material experiences plastic deformation, Alexander et al. [4] assigned HEL of SLG to be around 3.5 GPa since with no shear resistance, even the smallest shear stress will lead to plastic deformation. The highly pulverized material under the flyer in our experiments should result in the generation of such shear stresses. The material thus flows like a fluid under these conditions. Video recordings of in-situ compression loading of SLG pillars in a SEM chamber captured this remarkable fluid-like deformation in our previous work [6]. This resulted in the samples displaying extreme ductility with strain to failure exceeding 60%. In the dynamic experiments reported here the energy supply for such deformation is shut off at 8–16 ns depending upon the flyer thickness.

The occurrence of phase transformation within such a short duration is consistent with the MD simulation work of Shen et al. [21] in fused silica who report Stishovite nucleation to occur in 0.2 ns with subsequent grain growth occurring at 6 nm-ns⁻¹. Grujicic et al. [22] also observed an increase in the Si coordination number from 4 to 5 in a matter of 10 ps in a SLG sample that was shocked to 4 GPa. They however did not observe any Stishovite nucleation. These short durations suggest that such transformations arise from local correlated motions of atoms as opposed to longer length scale diffusive rearrangements. Dremin and Breusov [23] explain how fluid-like material flow upon plastic deformation provides transport of the atoms to the nuclei of the new phase to allow atomic intermixing and growth of the nucleated phase. This large-scale diffusion-like movement is accomplished through plastic deformation albeit at extremely short durations in the absence of regular diffusion. According to this scheme, when two layers of a substance are displaced relative to one another, on account of fluid-like plastic flow, the nuclei of a new phase located between them, can be regarded as a kind of a roller about which oscillations are executed. Since the time required for the rearrangement of electron shells (10^{-13} to 10^{-14} s) is much shorter than the time required for contact between atoms (10^{-12} s) , it follows that all atoms in their weak chemical bonding states passing in the immediate vicinity of the nucleus/crystallization centers have sufficient time to combine with the latter forming the new phase. Thus, in contrast to the usual diffusional growth of crystallization centers, in which each atom must find its way to the new phase, pushing apart its neighbors with the available thermal energy, the formation of the new phase during shock compression occurs by transport of the entire mass of the initial phase, by plastic flow, to the vicinity of the crystallization centers or activated complexes. The required atoms then combine selectively with the particles of the new phase, thus undergoing continuous growth during this process.

The aforesaid process also controls the mobility of both the highly mobile Na⁺ and Ca²⁺ ions in SLG to form dissimilar Na\\Ca pairs [24] to form regions of pure silica from which the Stishovite crystals can be nucleated. The large compositional difference between the amorphous SLG (SiO₂-NaO₂-CaO-....) and crystalline Stishovite (SiO₂) also assists in the diffusion process [25,26].

The low-pressure for observing Stishovite nucleation in SLG can be attributed to its more open and weaker network structure compared to fused silica. When alkali oxides, such as Na₂O and CaO, are added to pure SiO₂ to form SLG, the existing Si-O bonds are broken to incorporate the added oxygen ions in the network while the cations (Na⁺ and Ca²⁺) remain close by to form the weaker ionic bonds. As a result, overall concentration of "non-bridging" oxygen ions increases, which are absent in the fused silica network [3].

In addition to the shear stress, shock-induced local temperature rise could have also driven the nucleation of the Stishovite nanocrystals in our experiments. Using MD simulations, Shen et al. [21] have shown that the nucleation and growth kinetics of the Stishovite phase are a strong function of the shock temperature. Specifically, they found that the dependence of the Stishovite nucleation rate on temperature could be expressed using the standard Volmer-Weber nucleation model as,

$$\dot{N} = A \left[exp \left(-\frac{\alpha T_m^2}{T(T_m - T)^2} \right) exp \left(-\frac{Q_n}{T} \right) \right] \eqno(2)$$

where, α and A are constants, Q_n is the activation energy, and T_m is the melting temperature. The rate of nucleation thus increases with the temperature, however, as the temperature ap-

P. Srivastava, K. Tanaka, B. Ramirez et al. Acta Materialia 215 (2021) 117124

proaches the melting point, the lower free energy released from nucleation provides a weaker driving foce for the phase transition [21]. Once nucleated, the subsequent grain growth rate follows the standard Arrhenius dependence. Based on the MD simulation results of Grujicic et al. [27], the temperature rise in our samples is expected to be in the 500-1200 K range. These are low values. However, movement of the atoms under shear stress, as discussed above, can lead to the formation of hot spots due to lattice friction where the temperature can be significantly higher than that predicted by the Hugoniot relations. This is similar to the "hotspot crystallization" to Stishovite observed in porous sandstone by Mansfeld et al. [28] which they attributed to frictional heating and melting, followed by rapid quenching in those localized hot spots. Zhao et al. [29] have provided an analytical model to estimate this shear-driven local temperature rise in shock-compressed boron carbide crystals and found it to be significantly higher (1500 K) than the bulk temperature rise (500 K) at 45 GPa of shock compression. MD simulations of Devries et al. [30] reproduced Zhao et al. results. They observed that when the alloy was shocked to ~70 GPa, the temperature at the hot spots shot above the melting point (~2000 K) while the bulk temperature remained below ~900 K. They attributed this local temperature rise as the main contributor towards the dramatic loss of shear strength and amorphization in boron carbide. Therefore, in light of these works, the local temperature rise at the nucleation sites in our SLG samples is also expected to influence Stishovite formation.

The nanosecond shock duration and subsequent cooling of the sample after recovery in our experiments directly influences the size and volume fraction of the crystals formed. *In-situ* time-resolved diffraction experiments of shocked fused silica by Gleason et al. [31] have shown that Stishovite crystals revert to amorphous state within a fraction of nanosecond to 7 ns after the onset of the release wave, due to their limited thermal stability. Therefore, only trace amount of Stishovite crystals is expected to be present in the recovered samples. The presence of chemical impurities in SLG further limits the homogenous nucleation of Stishovite growth to only localized "cation-free" regions. This would explain why the Stishovite transformation is not uniform across our TEM samples and the largest crystal we obtained is only ~4 nm in size.

5. Summary

Soda-lime glass plates were shock loaded by impacting them using laser-generated and propelled 1mm-dia. Al microflyer plates of 25-50 µm thickness at 1-2.5 km/s. The stress state was determined by measuring the flyer speed, particle velocity, and shockwave speed by using a state-of-the-art PDV. The Hugoniot states obtained corresponded well with the conventional gas-gun launched plate impact experiments. The shocked samples were imaged using HRTEM and further analyzed using Selected Area Electron Diffraction and FFT analyses. All samples showed nucleation of 4 nm Stishovite crystals distributed within the amorphous SLG matrix. Surprisingly, a compressive stress of only 7 GPa corresponded to such nucleation events. Although this low stress falls within the reported Hugoniot Elastic Limit of SLG between 2.5 and 7 GPa, it is significantly below the crystallization threshold of 34 GPa observed for fused silica. The low nucleation stress as well as the small size of the nucleated crystals is attributed to the presence of cation impurities, high localized shear stress, and shear-driven temperature rise.

Declaration of Competing Interest

The authors declare that they have no known competing financial interests or personal relationships that could have appeared to influence the work reported in this paper.

Acknowledgments

The authors are particularly grateful to N. Bodzin for his assistance with TEM samples preparation by FIB.

Funding

This work was funded by the Office of Naval Research (ONR) under contract No. N00014-17-1-2490 for which we are grateful to Dr. Roshdy Barsoum of that agency.

References

- R.G. Barsoum, P.J. Dudt, S. Qadri, A.W. Ferrando, Polymorphic activity generated in soda-lime glass at hyper-velocity impact, in: Proceedings of the 29th International Symposium on Ballistics, 2016.
- [2] J.E. Gorfain, C.S Alexander, and C.T. Key. "High-pressure shock response and phase transition of soda-lime glass." AIP Conf. Proc., vol. 2272, no. 1, p. 100011.
- [3] C.S Alexander, L.C. Chhabildas, W.D. Reinhart, D.W. Templeton, Changes to the shock response of fused quartz due to glass modification, Int. J. Impact Eng. 35 (12) (2008) 1376–1385
- [4] P. Renganathan, T.S. Duffy, Y.M. Gupta, Hugoniot states and optical response of soda lime glass shock compressed to 120GPa, J. Appl. Phys. 127 (20) (2020) 205901
- [5] C.S Alexander, L.C. Chhabildas, D.W. Templeton, The Hugoniot Elastic Limit of soda-lime glass, AIP Conf. Proc. 955 (1) (2007) 733–738 American institute of physics.
- [6] M. Pozuelo, J. Lefebvre, P. Srivastava, V. Gupta, Stishovite formation at very low pressures in soda-lime glass, Scr. Mater. 171 (2019) 6–9.
- [7] K.E. Brown, W.L. Shaw, X. Zheng, D.D. Dlott, Simplified laser-driven flyer plates for shock compression science, Rev. Sci. Instrum. 83 (10) (2012) 103901.
- [8] A.D. Curtis, D.D. Dlott, Dynamics of shocks in laser-launched flyer plates probed by photon doppler velocimetry, J. Phys. Conf. Ser. 500 (19) (2014) 192002 IOP Publishing.
- [9] A.A. Banishev, W.L. Shaw, W.P. Bassett, D.D. Dlott, High-speed laser-launched flyer impacts studied with ultrafast photography and velocimetry, J. Dyn. Behav. Mater. 2 (2) (2016) 194–206.
- [10] H. Fujiwara, K. Brown, D. Dlott, A thin-film Hugoniot measurement using a laser-driven flyer plate, AIP Conf. Proc. 1426 (1) (2012) 382–385 American Institute of Physics.
- [11] D.P. Dandekar, Shock, release, and tension response of soda lime glass, AIP Conf. Proc. 429 (1) (1998) 525–528 American institute of physics.
- [12] N.K. Bourne, Z. Rosenberg, The dynamic response of soda-lime glass, AIP Conf. Proc. 370 (1) (1996) 567–572 American Institute of Physics.
- [13] T. Kobayashi, T. Sekine, O.V. Fat'yanov, E. Takazawa, Q.Y. Zhu, Radiation temperatures of soda-lime glass in its shock-compressed liquid state, J. Appl. Phys. 83 (3) (1998) 1711–1716.
- [14] S.P. Marsh, LASL Shock Hugoniot Data, 5, University of California Press, 1980.
- [15] S.N. Luo, J.L. Mosenfelder, PD. Asimow, TJ. Ahrens, Direct shock wave loading of Stishovite to 235 GPa: implications for perovskite stability relative to an oxide assemblage at lower mantle conditions, Geophys. Res. Lett. 29 (14) (2002) 36-1-36-4.
- [16] W.Q. Huang, S.R. Liu, Z.M. Huang, T.G Dong, G. Wang, C.J. Qin, Magic electron affection in preparation process of silicon nanocrystal, Sci. Rep. 5 (1) (2015)
- [17] S.J. Tracy, S.J. Turneaure, T.S. Duffy, In situ X-ray diffraction of shock-compressed fused silica, Phys. Rev. Lett. 120 (13) (2018) 135702.
- [18] S. Sundaram, R.J. Clifton, The influence of a glassy phase on the high strain rate response of a ceramic, Mech. Mater. 29 (3-4) (1998) 233–251.
- [19] R.J. Clifton, Response of materials under dynamic loading, Int. J. Solids Struct. 37 (1-2) (2000) 105–113.
- [20] R.J. Clifton, M. Mello, N.S. Brar, Effect of shear on failure waves in soda lime glass, AIP Conf. Proc. 429 (1) (1998) 521–524 American institute of physics.
- [21] Y. Shen, S.B. Jester, T. Qi, E.J. Reed, Nanosecond homogeneous nucleation and crystal growth in shock-compressed SiO₂.", Nat. Mater. 15 (1) (2016) 60–65.
- [22] M. Grujicic, W.C. Bell, P.S. Glomski, B. Pandurangan, B.A. Cheeseman, C. Fountzoulas, P. Patel, Multi-length scale modeling of high-pressure-induced phase transformations in soda-lime glass, J. Mater. Eng. Perform. 20 (7) (2011) 1144–1156.
- [23] A.N. Dremin, O.N. Breusov, Processes occurring in solids under the action of powerful shock waves, Russ. Chem. Rev. 37 (5) (1968) 392.
- [24] S.K. Lee, J.F. Stebbins, Nature of cation mixing and ordering in Na-Ca silicate glasses and melts, J. Phys. Chem. B 107 (14) (2003) 3141–3148.
- [25] C.A. Pampillo, H.S. Chen, Comprehensive plastic deformation of a bulk metallic glass, Mater. Sci. Eng. 13 (2) (1974) 181–188.
- [26] F.M Ernsberger, Role of densification in deformation of glasses under point loading, J. Am. Ceram. Soc. 51 (10) (1968) 545–547.
- [27] M. Grujicic, W.C. Bell, B. Pandurangan, B.A. Cheeseman, C. Fountzoulas, P. Patel, Molecular-level simulations of shock generation and propagation in soda-lime glass, J. Mater. Eng. Perform. 21 (8) (2012) 1580–1590.

P. Srivastava, K. Tanaka, B. Ramirez et al.

- [28] U. Mansfeld, F. Langenhorst, M. Ebert, A. Kowitz, R.T. Schmitt, Microscopic evidence of stishovite generated in low-pressure shock experiments on porous sandstone: constraints on its genesis, Meteorit. Planet. Sci. 52 (7) (2017) 1449–1464.
- [29] S. Zhao, B. Kad, B.A. Remington, J.C. LaSalvia, C.E. Wehrenberg, K.D. Behler, M.A. Meyers, Directional amorphization of boron carbide subjected to laser shock compression, in: Proceedings of the National Academy of Sciences, 113, 2016, pp. 12088–12093.
- [30] M. Devries, G. Subhash, A. Awasthi, Shocked ceramics melt: an atomistic analysis of thermodynamic behavior of boron carbide, Phys. Rev. B 101 (14) (2020) 144107.
- [31] A.E. Gleason, C.A. Bolme, H.J. Lee, B. Nagler, E. Galtier, R.G. Kraus, R. Sandberg, W. Yang, F. Langenhorst, W.L. Mao, Time-resolved diffraction of shock-released SiO₂ and diaplectic glass formation, Nat. Commun. 8 (1) (2017) 1–6.